

# Probing New Physics through $B$ Mixing: Status, Benchmarks and Prospects

Patricia Ball<sup>a,b</sup> and Robert Fleischer<sup>b</sup>

<sup>a</sup> *IPPP, Department of Physics, University of Durham, Durham DH1 3LE, UK*

<sup>b</sup> *Theory Division, Department of Physics, CERN, CH-1211 Geneva 23, Switzerland*

## Abstract

As is well known,  $B_{d,s}^0-\bar{B}_{d,s}^0$  mixing offers a profound probe into the effects of physics beyond the Standard Model. The data obtained at the  $e^+e^- B$  factories have already provided valuable insights into the  $B_d$ -meson system, and very recently also the  $B_s^0-\bar{B}_s^0$  oscillation frequency  $\Delta M_s$  has been measured at the Tevatron. We give a critical discussion of the interpretation of these data in terms of model-independent new-physics parameters. We address in particular the impact of the uncertainties of the relevant input parameters, set benchmarks for their accuracies as required by future precision measurements at the LHC, and explore the prospects for new CP-violating effects in the  $B_s$  system. To complement our model-independent analysis, we also discuss the constraints imposed by the CDF measurement of  $\Delta M_s$  on popular models of new physics, namely scenarios with an extra  $Z'$  boson and supersymmetry. We find that the new data still leave sizeable room for new-physics contributions to  $B_s^0-\bar{B}_s^0$  mixing, which could be detected at the LHC.



# 1 Introduction

One of the most promising ways to detect the effects of new physics (NP) on  $B$  decays is to look for deviations of flavour-changing neutral-current (FCNC) processes from their Standard Model (SM) predictions; FCNC processes only occur at the loop-level in the SM and hence are particularly sensitive to NP virtual particles and interactions. A prominent example that has received extensive experimental and theoretical attention is  $B_q^0\text{--}\bar{B}_q^0$  mixing ( $q \in \{d, s\}$ ), which, in the SM, is due to box diagrams with  $W$ -boson and up-type quark exchange. In the language of effective field theory, these diagrams induce an effective Hamiltonian, which causes  $B_q^0$  and  $\bar{B}_q^0$  mesons to mix and generates a  $\Delta B = 2$  transition:

$$\langle B_q^0 | \mathcal{H}_{\text{eff}}^{\Delta B=2} | \bar{B}_q^0 \rangle = 2M_{B_q} M_{12}^q, \quad (1)$$

where  $M_{B_q}$  is the  $B_q$ -meson mass. Thanks to  $B_q^0\text{--}\bar{B}_q^0$  mixing, an initially present  $B_q^0$  state evolves into a time-dependent linear combination of  $B_q^0$  and  $\bar{B}_q^0$  flavour states. The oscillation frequency of this phenomenon is characterized by the mass difference of the “heavy” and “light” mass eigenstates,

$$\Delta M_q \equiv M_{\text{H}}^q - M_{\text{L}}^q = 2|M_{12}^q|, \quad (2)$$

and the CP-violating mixing phase

$$\phi_q = \arg M_{12}^q, \quad (3)$$

which enters “mixing-induced” CP violation. The mass difference  $\Delta M_q$  can be – and has been – measured from the proper-time distribution of  $B_q^0$  candidates identified through their decays into (mostly) flavour-specific modes, after having been tagged as mixed or unmixed. The current experimental results are

$$\Delta M_d = (0.507 \pm 0.004) \text{ ps}^{-1}, \quad \Delta M_s = [17.33_{-0.21}^{+0.42}(\text{stat}) \pm 0.07(\text{syst})] \text{ ps}^{-1}, \quad (4)$$

where the value of  $\Delta M_d$  is the world average quoted by the “Heavy Flavour Averaging Group” (HFAG) [1]. Concerning  $\Delta M_s$ , only lower bounds were available for many years from the LEP experiments at CERN and SLD at SLAC [2]. Since the currently operating  $e^+e^-$   $B$  factories run at the  $\Upsilon(4S)$  resonance, which decays into  $B_{u,d}$ , but not into  $B_s$  mesons, the  $B_s$  system cannot be explored by the BaBar and Belle experiments. However, plenty of  $B_s$  mesons are produced at the Tevatron (and later on will be at the LHC), which – very recently – allowed the CDF collaboration to measure  $\Delta M_s$  with the result given above [3]; the D0 collaboration has provided, also very recently, a two-sided bound on  $\Delta M_s$  at the 90% C.L. [4]:

$$17 \text{ ps}^{-1} < \Delta M_s < 21 \text{ ps}^{-1}, \quad (5)$$

which is compatible with the CDF measurement and corresponds to a  $2.5\sigma$  signal at  $\Delta M_s = 19 \text{ ps}^{-1}$ . These new results from the Tevatron have already triggered a couple of phenomenological papers [5]–[11].

In the SM,  $M_{12}^q$  is given by

$$M_{12}^{q,\text{SM}} = \frac{G_{\text{F}}^2 M_W^2}{12\pi^2} M_{B_q} \hat{\eta}^B \hat{B}_{B_q} f_{B_q}^2 (V_{tq}^* V_{tb})^2 S_0(x_t), \quad (6)$$

where  $G_F$  is Fermi's constant,  $M_W$  the mass of the  $W$  boson,  $\hat{\eta}^B = 0.552$  a short-distance QCD correction (which is the same for the  $B_d^0$  and  $B_s^0$  systems) [12], whereas the “bag” parameter  $\hat{B}_{B_q}$  and the decay constant  $f_{B_q}$  are non-perturbative quantities.  $V_{tq}$  and  $V_{tb}$  are elements of the Cabibbo–Kobayashi–Maskawa (CKM) matrix [13, 14], and  $S_0(x_t \equiv \bar{m}_t^2/M_W^2) = 2.35 \pm 0.06$  with  $\bar{m}_t(m_t) = (164.7 \pm 2.8)$  GeV [15] is one of the “Inami–Lim” functions [16], describing the  $t$ -quark mass dependence of the box diagram with internal  $t$ -quark exchange; the contributions of internal  $c$  and  $u$  quarks are, by virtue of the Glashow–Iliopoulos–Maiani (GIM) mechanism [17], suppressed by  $(m_{u,c}/M_W)^2$ .

The mixing phases  $\phi_q$  can be measured from “mixing-induced” CP asymmetries. In the SM, one has

$$\phi_d^{\text{SM}} = 2\beta, \quad \phi_s^{\text{SM}} = -2\delta\gamma, \quad (7)$$

where  $\beta$  is the usual angle of the “conventional” unitarity triangle (UT) of the CKM matrix, while  $\delta\gamma$  characterizes another unitarity triangle [18] that differs from the UT through  $\mathcal{O}(\lambda^2)$  corrections in the Wolfenstein expansion [19].<sup>1</sup>

The purpose of this paper is to explore the possibility that  $B_q^0$ – $\bar{B}_q^0$  mixing is modified by NP contributions at the tree level and/or new particles in the loops. We shall find in particular that – despite the apparently strong constraints posed by the precise measurements of  $\Delta M_q$  in Eq. (4) – these results can contain potentially large NP contributions, which presently cannot be detected.

The outline of our paper is as follows: in Section 2, we collect the input parameters of our analysis and discuss the status of the relevant hadronic uncertainties. In Sections 3 and 4, we then focus on the  $B_d$ - and  $B_s$ -meson systems, respectively, and investigate, in a model-independent way, the size of possible NP contributions to  $\Delta M_q$  and  $\phi_q$  in the light of present and future experimental measurements and hadronic uncertainties. In this analysis, we consider also a scenario for the experimental and theoretical situation in the year 2010, and set benchmarks for the required accuracy of the relevant hadronic parameters. It turns out that the situation in the  $B_s$  system is more favourable than in the  $B_d$  system, and that still ample space for NP effects in  $B_s^0$ – $\bar{B}_s^0$  mixing is left, which could be detected at the LHC. In Section 5, we complement the model-independent discussion of Sections 3 and 4 by analyses of two specific scenarios for NP: models with an extra  $Z'$  boson and supersymmetry (SUSY) with an approximate alignment of quark and squark masses. We summarize our conclusions in Section 6.

## 2 Input Parameters and Hadronic Uncertainties

### 2.1 CKM Parameters

Before going into the details of  $B_q^0$ – $\bar{B}_q^0$  mixing and possible NP effects, let us first have a closer look at the relevant input parameters and their uncertainties. Throughout our analysis, we assume that the CKM matrix is unitary, and shall use this feature to express the CKM elements entering  $B_q^0$ – $\bar{B}_q^0$  mixing in terms of quantities that can be determined

---

<sup>1</sup>Throughout this paper, we use the phase convention for the CKM matrix advocated by the Particle Data Group [20], where the decay amplitudes of  $b \rightarrow c\bar{c}s$  processes carry essentially no CP-violating weak phase. Physical CP asymmetries are of course independent of the applied CKM phase convention, as shown explicitly in Ref. [21].

through tree-level processes of the SM. The key rôle is then played by  $|V_{cb}|$  and  $|V_{ub}|$ . The former quantity is presently known with 2% precision from semileptonic  $B$  decays; in this paper we shall use the value obtained in Ref. [22] from the analysis of leptonic and hadronic moments in inclusive  $b \rightarrow c\ell\bar{\nu}_\ell$  transitions [23]:

$$|V_{cb}| = (42.0 \pm 0.7) \cdot 10^{-3}; \quad (8)$$

this value agrees with that from exclusive decays.

The situation is less favourable with  $|V_{ub}|$ : there is a  $1\sigma$  discrepancy between the values from inclusive and exclusive  $b \rightarrow u\ell\bar{\nu}_\ell$  transitions [1]:

$$|V_{ub}|_{\text{incl}} = (4.4 \pm 0.3) \cdot 10^{-3}, \quad |V_{ub}|_{\text{excl}} = (3.8 \pm 0.6) \cdot 10^{-3}. \quad (9)$$

The error on  $|V_{ub}|_{\text{excl}}$  is dominated by the theoretical uncertainty of lattice and light-cone sum rule calculations of  $B \rightarrow \pi$  and  $B \rightarrow \rho$  transition form factors [24, 25], whereas for  $|V_{ub}|_{\text{incl}}$  experimental and theoretical errors are at par. We will use both results in our analysis.

Whereas any improvement of the error of  $|V_{cb}|$  will have only marginal impact on the analysis of  $B$  mixing, a reduction of the uncertainty of  $|V_{ub}|$  will be very relevant. As a benchmark scenario for the situation in 2010, we will assume that the central value of  $|V_{ub}|_{\text{incl}}$  gets confirmed and that its uncertainty will shrink to  $\pm 0.2 \cdot 10^{-3}$ , i.e. 5%, thanks to better statistics and an increased precision of theoretical predictions, for instance from further developments in the dressed gluon exponentiation [26].

## 2.2 Hadronic Mixing Parameters $f_{B_q} \hat{B}_{B_q}^{1/2}$

The next ingredient in the SM prediction for  $M_{12}^{q,\text{SM}}$  are the non-perturbative matrix elements  $f_{B_q}^2 \hat{B}_{B_q}$ . These parameters have been the subject of numerous lattice calculations, both quenched and unquenched, using various lattice actions and implementations of both heavy and light quarks. The current front runners are unquenched calculations with 2 and 3 dynamical quarks, respectively, and Wilson or staggered light quarks. Despite tremendous progress in recent years, the results still suffer from a variety of uncertainties which is important to keep in mind when interpreting and using lattice results. One particular difficulty in determining  $f_{B_d}$  is the chiral extrapolation needed to go to the physical  $d$ -quark mass.<sup>2</sup> Lattice calculations are usually performed at unphysically large  $u$ - and  $d$ -quark masses, as the simulation of dynamical fermions involves many inversions of the fermions' functional determinant in the path integral and is very dear in terms of CPU time. Therefore, an extrapolation, called the chiral extrapolation, in the light-quark masses from feasible to physical masses is necessary, which is done using the functional form predicted by chiral perturbation theory. Based on these arguments, the chiral extrapolation of  $\hat{B}_{B_d}$  to the physical limit is expected to be smooth, whereas that of  $f_{B_d}$  is potentially prone to logarithms [28], which leads to a considerable increase in the uncertainty. The most recent (unquenched) simulation by the JLQCD collaboration [29],

---

<sup>2</sup>Many lattice simulations do not distinguish between  $u$ - and  $d$ -quark masses and use  $m_{u,d} \equiv (m_u + m_d)/2$ . The physical value of the light-quark mass ratio is then  $m_{u,d}/m_s = 0.041 \pm 0.003$  from chiral perturbation theory [27].

with non-relativistic  $b$  quarks and two flavours of dynamical light (Wilson) quarks, yields  $f_{B_d} = (0.191 \pm 0.010_{-0.022}^{+0.012})$  GeV and

$$\begin{aligned} f_{B_d} \hat{B}_{B_d}^{1/2} \Big|_{\text{JLQCD}} &= (0.215 \pm 0.019_{-0.023}^{+0}) \text{ GeV}, \\ f_{B_s} \hat{B}_{B_s}^{1/2} \Big|_{\text{JLQCD}} &= (0.245 \pm 0.021_{-0.002}^{+0.003}) \text{ GeV}, \\ \xi_{\text{JLQCD}} \equiv \frac{f_{B_s} \hat{B}_{B_s}^{1/2}}{f_{B_d} \hat{B}_{B_d}^{1/2}} \Big|_{\text{JLQCD}} &= 1.14 \pm 0.06_{-0}^{+0.13}, \end{aligned} \quad (10)$$

where the first error includes uncertainties from statistics and various systematics, whereas the second, asymmetric error comes from the chiral extrapolation. Note that part of the systematic errors cancel in the ratio  $\xi$ . In this calculation, the ratio  $m_{u,d}/m_s$  was varied between 0.7 and 2.9.

More recently, (unquenched) simulations with three dynamical flavours have become possible using staggered quark actions. The HPQCD collaboration obtains  $f_{B_d} = (0.216 \pm 0.022)$  MeV [30], where a ratio of  $m_{u,d}/m_s$  as small as 0.125 could be achieved, due to the good chiral properties of the staggered action. This implies that the chiral extrapolation is less critical and the corresponding error much smaller. The quoted error on  $f_{B_q}$  is now dominated by yet uncalculated higher-order matching terms which are needed to match the (effective theory) lattice calculations to continuum QCD. Lacking any direct calculation of  $\hat{B}_{B_q}$  with three dynamical flavours, and in view of the fact that the bag parameter is likely to be less sensitive to chiral extrapolation, it has been suggested to combine the results of  $f_{B_q}$  from HPQCD with that of  $\hat{B}_{B_q}$  from JLQCD, yielding [31]:

$$\begin{aligned} f_{B_d} \hat{B}_{B_d}^{1/2} \Big|_{(\text{HP+JL})\text{QCD}} &= (0.244 \pm 0.026) \text{ GeV}, \\ f_{B_s} \hat{B}_{B_s}^{1/2} \Big|_{(\text{HP+JL})\text{QCD}} &= (0.295 \pm 0.036) \text{ GeV}, \\ \xi_{(\text{HP+JL})\text{QCD}} &= 1.210_{-0.035}^{+0.047}, \end{aligned} \quad (11)$$

where all errors are added in quadrature.

Although we shall use both (10) and (11) in our analysis, we would like to stress that the errors are likely to be optimistic. Apart from the issue of the chiral extrapolation discussed above, there is also the question of discretisation effects (JLQCD uses data obtained at only one lattice spacing) and the renormalisation of matrix elements (for lattice actions without chiral symmetry, the axial vector current is not conserved and  $f_{B_q}$  needs to be renormalised), which some argue should be done in a non-perturbative way [32]. Simulations with staggered quarks also face potential problems with unitarity, locality and an odd number of flavours (see, for instance, Ref. [33]). A confirmation of the HPQCD results by simulations using the (theoretically better understood) Wilson action with small quark masses will certainly be highly welcome.

Given this situation, we consider it not very likely that the errors on  $f_{B_q}$ ,  $\hat{B}_{B_q}$  and  $\xi$  will come down considerably in the near future. For our benchmark 2010 scenario, we hence will assume the values of hadronic parameters and uncertainties given in (11).

We are now well prepared for the discussion of  $B_q^0 - \bar{B}_q^0$  mixing.

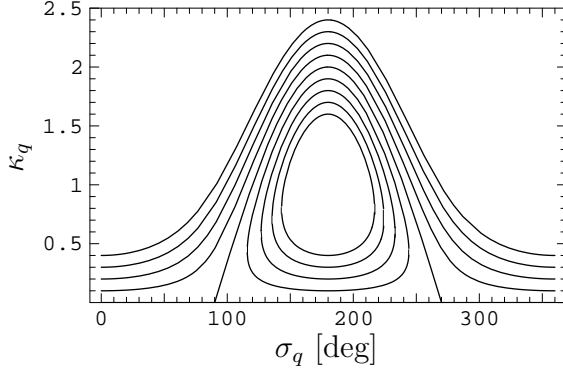


Figure 1: The dependence of  $\kappa_q$  on  $\sigma_q$  for values of  $\rho_q$  varied between 1.4 (most upper curve) and 0.6 (most inner curve), in steps of 0.1. The contours apply to both the  $q = d$  and the  $q = s$  system.

### 3 The $B_d$ -Meson System

#### 3.1 Model-Independent NP Parameters

Let us first have a closer look at the  $B_d^0-\bar{B}_d^0$  mixing parameters. In the presence of NP, the matrix element  $M_{12}^d$  can be written, in a model-independent way, as

$$M_{12}^d = M_{12}^{d,\text{SM}} \left( 1 + \kappa_d e^{i\sigma_d} \right),$$

where the real parameter  $\kappa_d \geq 0$  measures the “strength” of the NP contribution with respect to the SM, whereas  $\sigma_d$  is a new CP-violating phase; analogous formulae apply to the  $B_s$  system. The  $B_d$  mixing parameters then read

$$\Delta M_d = \Delta M_d^{\text{SM}} \left[ 1 + \kappa_d e^{i\sigma_d} \right], \quad (12)$$

$$\phi_d = \phi_d^{\text{SM}} + \phi_d^{\text{NP}} = \phi_d^{\text{SM}} + \arg(1 + \kappa_d e^{i\sigma_d}). \quad (13)$$

The experimental result for  $\Delta M_d$  and the theoretical prediction  $\Delta M_d^{\text{SM}}$  provide the following constraint on  $\kappa_d$  and  $\sigma_d$ :

$$\rho_d \equiv \left| \frac{\Delta M_d}{\Delta M_d^{\text{SM}}} \right| = \sqrt{1 + 2\kappa_d \cos \sigma_d + \kappa_d^2}, \quad (14)$$

which determines, for instance,  $\kappa_d$  as function of  $\sigma_d$ :

$$\kappa_d = -\cos \sigma_d \pm \sqrt{\rho_d^2 - \sin^2 \sigma_d}. \quad (15)$$

In Fig. 1, we illustrate the corresponding contours in the  $\sigma_d$ - $\kappa_d$  plane for values of  $\rho_d$  between 0.6 and 1.4, varied in steps of 0.1. Interestingly enough, a value of  $\rho_d$  smaller than 1 imposes a constraint on the weak NP phase  $\sigma_d$ :

$$\pi - \arcsin \rho_d \leq \sigma_d \leq \pi + \arcsin \rho_d. \quad (16)$$

### 3.2 The SM Prediction for $\Delta M_d$

In order to make use of these constraints, one needs to know the SM prediction  $\Delta M_d^{\text{SM}}$ . In particular, one has to make sure that the parameters entering  $M_{12}^{d,\text{SM}}$ , Eq. (6), are free from NP. This can be achieved, to very good accuracy, by expressing the relevant CKM factor in  $\Delta M_d^{\text{SM}}$  in terms of parameters measured in tree-level processes. To this end, we use the Wolfenstein parametrization [19], as generalized in Ref. [34], and the unitarity of the CKM matrix to write

$$|V_{td}^* V_{tb}| = |V_{cb}| \lambda \sqrt{1 - 2R_b \cos \gamma + R_b^2}. \quad (17)$$

Here the quantity  $R_b$  is given by

$$R_b \equiv \left(1 - \frac{\lambda^2}{2}\right) \frac{1}{\lambda} \left| \frac{V_{ub}}{V_{cb}} \right| = \sqrt{\bar{\rho}^2 + \bar{\eta}^2}, \quad (18)$$

with

$$\bar{\rho} = (1 - \lambda^2/2)\rho = R_b \cos \gamma, \quad \bar{\eta} = (1 - \lambda^2/2)\eta = R_b \sin \gamma; \quad (19)$$

$R_b$  measures one side of the UT, and  $\gamma$  denotes the usual UT angle.

As we saw in Section 2,  $|V_{cb}|$  and  $|V_{ub}|$  can be determined from semileptonic  $B$  decays, which arise at tree level in the SM and hence are very robust with respect to NP effects. A similar comment applies to the Wolfenstein parameter  $\lambda \equiv |V_{us}|$  [19, 34], which can be determined, for instance, from  $K \rightarrow \pi \ell \bar{\nu}_\ell$  decays. Using the values of  $|V_{cb}|$  and  $|V_{ub}|$  discussed in Section 2 and  $\lambda = 0.225 \pm 0.001$  [35], we obtain

$$R_b^{\text{incl}} = 0.45 \pm 0.03, \quad R_b^{\text{excl}} = 0.39 \pm 0.06, \quad (20)$$

where the labels ‘‘incl’’ and ‘‘excl’’ refer to the determinations of  $|V_{ub}|$  through inclusive and exclusive  $b \rightarrow u \ell \bar{\nu}_\ell$  transitions, respectively.

The angle  $\gamma$  can be determined in a variety of ways through CP-violating effects in pure tree decays of type  $B \rightarrow D^{(*)} K^{(*)}$  [36]. Using the present  $B$ -factory data, the following results were obtained through a combination of various methods:

$$\gamma|_{D^{(*)}K^{(*)}} = \begin{cases} (62_{-25}^{+35})^\circ & \text{(CKMfitter collaboration [37]),} \\ (65 \pm 20)^\circ & \text{(UTfit collaboration [38]).} \end{cases} \quad (21)$$

A more precise value for  $\gamma$  was obtained in Ref. [39], from the  $B$ -factory data on CP asymmetries in  $B_d^0 \rightarrow \pi^+ \pi^-$  and  $B_d^0 \rightarrow \pi^- K^+$  decays, which receive both tree and penguin contributions:

$$\gamma|_{\pi^+ \pi^-, \pi^- K^+} = (73.9_{-6.5}^{+5.8})^\circ. \quad (22)$$

Within the NP scenario of modified electroweak penguins considered in Ref. [39], (22) is not affected by NP effects. The central value of (22) is higher than that of (21), but both results are perfectly consistent because of the large errors of the  $B \rightarrow D^{(*)} K^{(*)}$  determinations. An even larger value of  $\gamma$  in the ballpark of  $80^\circ$  was recently extracted from  $B \rightarrow \pi \pi$  data with the help of ‘‘soft collinear effective theory’’ (SCET) [40].

In our analysis, we use the UTfit value

$$\gamma = (65 \pm 20)^\circ. \quad (23)$$



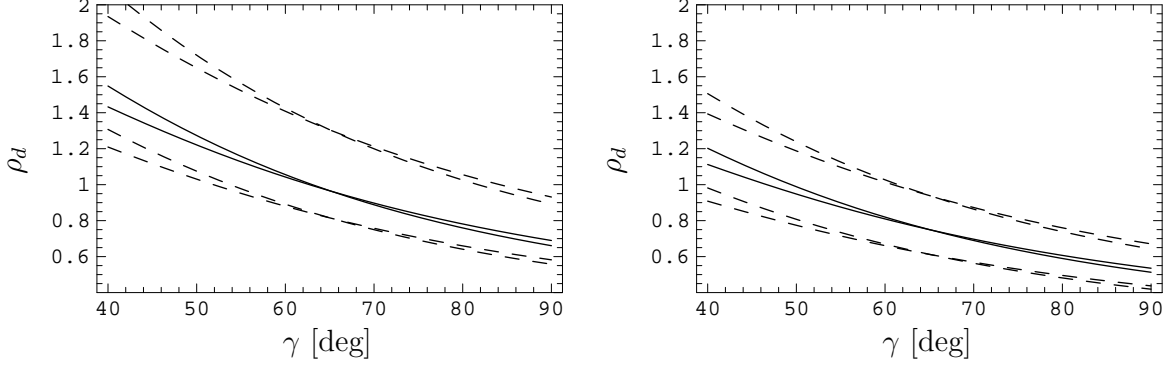


Figure 2: The dependence of  $\rho_d$  on  $\gamma$  for  $R_b = (0.39, 0.45)$  and various values of  $f_{B_d} \hat{B}_{B_d}^{1/2}$ . Left panel: JLQCD results (10):  $f_{B_d} \hat{B}_{B_d}^{1/2} = 0.215$  GeV (solid lines),  $f_{B_d} \hat{B}_{B_d}^{1/2} = (0.185, 0.234)$  GeV (dashed lines). Right panel: ditto for (HP+JL)QCD results (11):  $f_{B_d} \hat{B}_{B_d}^{1/2} = 0.244$  GeV (solid lines),  $f_{B_d} \hat{B}_{B_d}^{1/2} = (0.218, 0.270)$  GeV (dashed lines).

With the help of (8), (17) and (20), we then obtain

$$|V_{td}^* V_{tb}|_{\text{incl}} = (8.6 \pm 1.5) \cdot 10^{-3}, \quad |V_{td}^* V_{tb}|_{\text{excl}} = (8.6 \pm 1.3) \cdot 10^{-3}, \quad (24)$$

where the uncertainty is dominated by that of the angle  $\gamma$ .

For our 2010 benchmark scenario, we assume that the central value of  $\gamma$  will settle at  $70^\circ$ , and that the error will shrink to  $\pm 5^\circ$  thanks to strategies using pure tree decays of  $B_{u,d}$  and  $B_s$  mesons for the determination of  $\gamma$ , which can be implemented at the LHC. In fact, a statistical accuracy of  $\sigma_{\text{stat}}(\gamma) \approx 2.5^\circ$  is expected at LHCb after 5 years of taking data [41].

For the convenience of the reader, we summarise all CKM input parameters, as well as their counterparts for the  $B_s$  system to be discussed in Section 4, in Tab. 1; in Tab. 2, we give the input data for our 2010 scenario.

In Fig. 2, we illustrate the dependence of  $\rho_d$  defined in (14) on  $\gamma$ ,  $R_b$  and  $f_{B_d} \hat{B}_{B_d}^{1/2}$ . It is evident that  $\rho_d$  depends rather strongly on  $\gamma$  and  $f_{B_d} \hat{B}_{B_d}^{1/2}$ , but less so on  $R_b$ . For the two different lattice results, we obtain

$$\begin{aligned} \Delta M_d^{\text{SM}} \Big|_{\text{JLQCD}} &= \left[ 0.52 \pm 0.17(\gamma, R_b)_{+0.13}^{-0.09} (f_{B_d} \hat{B}_{B_d}^{1/2}) \right] \text{ps}^{-1}, \\ \rho_d \Big|_{\text{JLQCD}} &= 0.97 \pm 0.33(\gamma, R_b)_{+0.26}^{-0.17} (f_{B_d} \hat{B}_{B_d}^{1/2}), \\ \Delta M_d^{\text{SM}} \Big|_{(\text{HP+JL})\text{QCD}} &= \left[ 0.69 \pm 0.13(\gamma, R_b) \pm 0.08(f_{B_d} \hat{B}_{B_d}^{1/2}) \right] \text{ps}^{-1}, \\ \rho_d \Big|_{(\text{HP+JL})\text{QCD}} &= 0.75 \pm 0.25(\gamma, R_b) \pm 0.16(f_{B_d} \hat{B}_{B_d}^{1/2}), \end{aligned} \quad (25)$$

where we made explicit the errors arising from the uncertainties of  $(\gamma, R_b)$  and  $f_{B_d} \hat{B}_{B_d}^{1/2}$ . These results are compatible with the SM value  $\rho_d = 1$ , but suffer from considerable uncertainties, which presently leave sizeable room for NP contributions to  $\Delta M_d$ ; we shall quantify below the allowed values of  $\kappa_d$  and  $\sigma_d$  following from the contours in Fig. 1.

| Parameter                         | Value                          | Ref.     | Remarks                                      |
|-----------------------------------|--------------------------------|----------|--|
| $\lambda$                         | $0.225 \pm 0.001$              | [35]     | CKM05 average                                |
| $ V_{cb} $                        | $(42.0 \pm 0.7) \cdot 10^{-3}$ | [22]     | inclusive $b \rightarrow c l \bar{\nu}_\ell$ |
| $ V_{ub} _{\text{incl}}$          | $(4.4 \pm 0.3) \cdot 10^{-3}$  | [1]      | our average                                  |
| $ V_{ub} _{\text{excl}}$          | $(3.8 \pm 0.6) \cdot 10^{-3}$  | [1]      | our average                                  |
| $\gamma$                          | $(65 \pm 20)^\circ$            | [38]     | UTfit average                                |
| $R_b^{\text{incl}}$               | $0.45 \pm 0.03$                | Eq. (18) |  |
| $R_b^{\text{excl}}$               | $0.39 \pm 0.06$                | Eq. (18) |  |
| $R_t$                             | $0.91 \pm 0.16$                | Eq. (39) | error dominated by $\gamma$                  |
| $ V_{td}^* V_{tb} _{\text{incl}}$ | $(8.6 \pm 1.5) \cdot 10^{-3}$  | Eq. (17) | error dominated by $\gamma$                  |
| $ V_{td}^* V_{tb} _{\text{excl}}$ | $(8.6 \pm 1.3) \cdot 10^{-3}$  | Eq. (17) | error dominated by $\gamma$                  |
| $ V_{ts}^* V_{tb} $               | $(41.3 \pm 0.7) \cdot 10^{-3}$ | Eq. (35) |  |
| $\beta_{\text{incl}}$             | $(26.7 \pm 1.9)^\circ$         | Eq. (32) | error dominated by $R_b$                     |
| $\beta_{\text{excl}}$             | $(22.9 \pm 3.8)^\circ$         | Eq. (32) | error dominated by $R_b$                     |

Table 1: CKM parameters used in our analysis. All parameters are determined using input from tree-level processes only and the unitarity of the CKM matrix.

| Parameter                     | Value                           |
|-------------------------------|---------------------------------|
| $\lambda$                     | $0.225 \pm 0.001$               |
| $ V_{cb} $                    | $(42.0 \pm 0.7) \cdot 10^{-3}$  |
| $ V_{ub} $                    | $(4.4 \pm 0.2) \cdot 10^{-3}$   |
| $\gamma$                      | $(70 \pm 5)^\circ$              |
| $R_b$                         | $0.45 \pm 0.02$                 |
| $R_t$                         | $0.95 \pm 0.04$                 |
| $ V_{td}^* V_{tb} $           | $(8.9 \pm 0.4) \cdot 10^{-3}$   |
| $ V_{ts}^* V_{tb} $           | $(41.3 \pm 0.7) \cdot 10^{-3}$  |
| $\beta$                       | $(26.6 \pm 1.2)^\circ$          |
| $f_{B_d} \hat{B}_{B_d}^{1/2}$ | $(0.244 \pm 0.026) \text{ GeV}$ |
| $f_{B_s} \hat{B}_{B_s}^{1/2}$ | $(0.295 \pm 0.036) \text{ GeV}$ |
| $\rho_d$                      | $0.69 \pm 0.16$                 |
| $\rho_s$                      | $0.74 \pm 0.18$                 |
| $\xi$                         | $1.210_{-0.035}^{+0.047}$       |
| $\rho_s/\rho_d$               | $1.07 \pm 0.12$                 |

Table 2: Benchmark values and uncertainties for CKM and hadronic parameters in 2010.

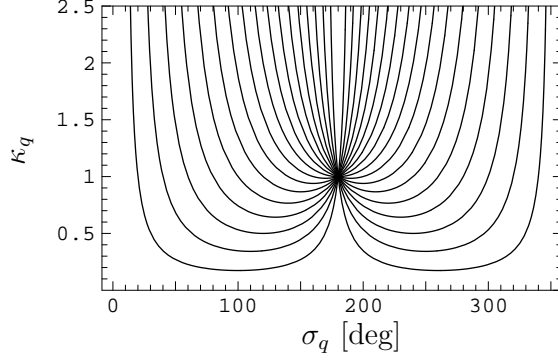


Figure 3: The dependence of  $\kappa_q$  on  $\sigma_q$  for values of  $\phi_q^{\text{NP}}$  varied between  $\pm 10^\circ$  (lower curves) and  $\pm 170^\circ$  in steps of  $10^\circ$ : the curves for  $0^\circ < \sigma_q < 180^\circ$  and  $180^\circ < \sigma_q < 360^\circ$  correspond to positive and negative values of  $\phi_q^{\text{NP}}$ , respectively. The contours apply to both the  $q = d$  and the  $q = s$  system.

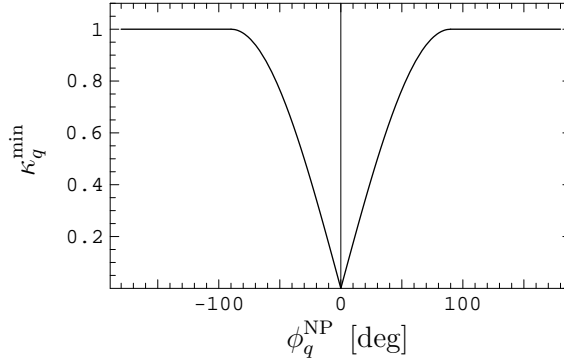


Figure 4: The minimum value  $\kappa_q^{\text{min}}$  of  $\kappa_q$  as function of the NP mixing phase  $\phi_q^{\text{NP}}$ .

### 3.3 Constraints on NP through CP Violation: $\phi_d$

The second constraint on the allowed values of  $\kappa_d$  and  $\sigma_d$  is provided by the experimental value of the  $B_d$  mixing phase  $\phi_d = \phi_d^{\text{SM}} + \phi_d^{\text{NP}}$ . Using (13), a given value of  $\phi_d^{\text{NP}}$  allows one to determine  $\kappa_d$  as a function of  $\sigma_d$  with the help of the following expressions, which hold again in the general case  $q \in \{d, s\}$ :

$$\kappa_q = \frac{\tan \phi_q^{\text{NP}}}{\sin \sigma_q - \cos \sigma_q \tan \phi_q^{\text{NP}}}, \quad (26)$$

$$\sin \phi_q^{\text{NP}} = \frac{\kappa_q \sin \sigma_q}{\sqrt{1 + 2\kappa_q \cos \sigma_q + \kappa_q^2}}, \quad \cos \phi_q^{\text{NP}} = \frac{1 + \kappa_q \cos \sigma_q}{\sqrt{1 + 2\kappa_q \cos \sigma_q + \kappa_q^2}}. \quad (27)$$

In Fig. 3, we illustrate the corresponding contours for various values of  $\phi_q^{\text{NP}}$ . Note in particular that  $\kappa_q$  is bounded from below for any given value of  $\phi_q^{\text{NP}} \neq 0$ . The relation between the allowed values of  $\phi_q^{\text{NP}}$  and  $\kappa_q$  is given by

$$\phi_q^{\text{NP, max(min)}} = \arg \left\{ 1 + \kappa_q \left( -\kappa_q^2 \pm i\sqrt{1 - \kappa_q^2} \right) \right\}, \quad (28)$$

i.e. for any non-zero value of  $\phi_q^{\text{NP}}$ ,  $\kappa_q$  must be larger than the minimum value plotted in Fig. 4.

In order to make use of these theoretically clean contours, one needs to determine the NP phase  $\phi_d^{\text{NP}}$ . As is well known,  $\phi_d$  can be experimentally accessed in the mixing-induced CP asymmetry of the “golden” decay  $B_d^0 \rightarrow J/\psi K_S$  (and similar  $b \rightarrow c\bar{c}s$  charmonium modes) [42]. The most recent average of the  $B$ -factory data for such transitions obtained by HFAG is [1]

$$(\sin \phi_d)_{c\bar{c}s} = 0.687 \pm 0.032. \quad (29)$$

In principle, this quantity could be affected by NP contributions to both  $B_d^0\text{--}\bar{B}_d^0$  mixing and  $b \rightarrow c\bar{c}s$  decay amplitudes [43, 44]. A probe of the latter effects is provided by decays like  $B_d \rightarrow D\pi^0, D\rho^0, \dots$ , which are pure tree decays and do not receive any penguin contributions. If the neutral  $D$  mesons are observed through their decays into CP eigenstates  $D_{\pm}$ , these decays allow an extremely clean determination of the “true” value of  $\sin \phi_d$  [45]. A possible discrepancy with  $(\sin \phi_d)_{c\bar{c}s}$  would be attributed to NP contributions to the  $b \rightarrow c\bar{c}s$  decay amplitudes. Consequently, detailed feasibility studies for the exploration of  $B_d \rightarrow D\pi^0, D\rho^0, \dots$  modes at a super- $B$  factory are strongly encouraged. In this paper, however, we assume that NP effects entering decay amplitudes are negligible. Eq. (13) then gives the following expression:

$$(\sin \phi_d)_{c\bar{c}s} \equiv \sin \phi_d = \sin(2\beta + \phi_d^{\text{NP}}). \quad (30)$$

The experimental value (29) yields the twofold solution

$$\phi_d = (43.4 \pm 2.5)^\circ \quad \vee \quad (136.6 \pm 2.5)^\circ, \quad (31)$$

where the latter result is in dramatic conflict with global CKM fits and would require a large NP contribution to  $B_d^0\text{--}\bar{B}_d^0$  mixing [46, 47]. However, experimental information on the sign of  $\cos \phi_d$  rules out a negative value of this quantity at greater than 95% C.L. [36], so that we are left with  $\phi_d = (43.4 \pm 2.5)^\circ$ .

The SM prediction of the mixing phase,  $\phi_d^{\text{SM}} = 2\beta$ , Eq. (7), can easily be obtained in terms of the tree-level quantities  $R_b$  and  $\gamma$ , as

$$\sin \beta = \frac{R_b \sin \gamma}{\sqrt{1 - 2R_b \cos \gamma + R_b^2}}, \quad \cos \beta = \frac{1 - R_b \cos \gamma}{\sqrt{1 - 2R_b \cos \gamma + R_b^2}}. \quad (32)$$

Using Eq. (13), the experimental value of  $\phi_d$  can then immediately be converted into a result for the NP phase  $\phi_d^{\text{NP}}$ , which depends on  $\gamma$  and  $R_b$  as illustrated in Fig. 5. It is evident that the dependence of  $\phi_d^{\text{NP}}$  on  $\gamma$  is very small and that  $R_b$  plays actually the key rôle for its determination. Hence, we have a situation complementary to that shown in Fig. 2, where the main dependence was on  $\gamma$ . The parameters collected in Tab. 1 yield

$$\phi_d^{\text{SM}}|_{\text{incl}} = (53.4 \pm 3.8)^\circ, \quad \phi_d^{\text{SM}}|_{\text{excl}} = (45.8 \pm 7.6)^\circ, \quad (33)$$

corresponding to

$$\phi_d^{\text{NP}}|_{\text{incl}} = -(10.1 \pm 4.6)^\circ, \quad \phi_d^{\text{NP}}|_{\text{excl}} = -(2.5 \pm 8.0)^\circ; \quad (34)$$

results of  $\phi_d^{\text{NP}} \approx -10^\circ$  were also recently obtained in Refs. [39, 48]. Note that the emergence of a non-zero value of  $\phi_d^{\text{NP}}$  is caused by the large value of  $|V_{ub}|$  from inclusive

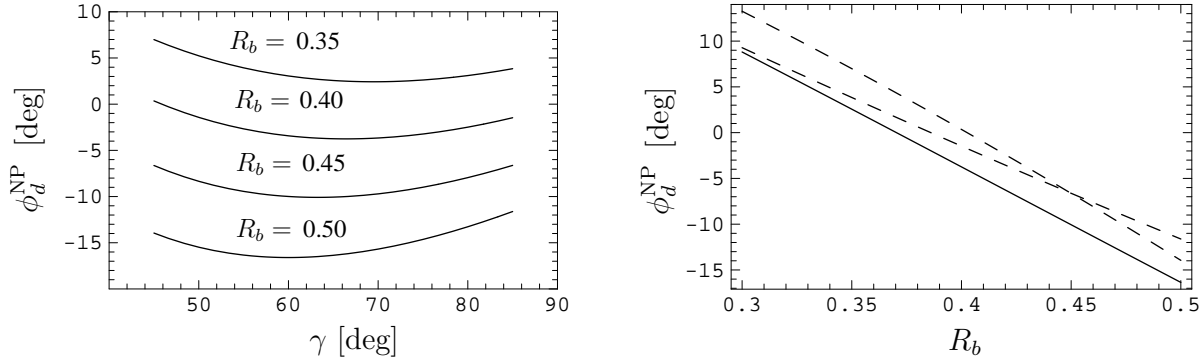


Figure 5: The determination of  $\phi_d^{\text{NP}}$  for  $\phi_d = 43.4^\circ$ . Left panel:  $\phi_d^{\text{NP}}$  as a function of  $\gamma$  for various values of  $R_b$ . Right panel:  $\phi_d^{\text{NP}}$  as a function of  $R_b$  for various values of  $\gamma$  (solid line:  $\gamma = 65^\circ$ , dashed lines:  $\gamma = (45^\circ, 85^\circ)$ ).

semileptonic decays, but that  $\phi_d^{\text{NP}}$  is compatible with zero for  $|V_{ub}|$  from exclusive decays. The consequences of the presence of a small NP phase  $\phi_d^{\text{NP}} \approx -10^\circ$  are rather dramatic: from Fig. 4, one reads off the sizeable lower bound  $\kappa_d \gtrsim 0.17$ . Although this result hinges on the value of  $|V_{ub}|_{\text{incl}}$ , and hence presently is not conclusive, the underlying reasoning also applies to the  $B_s$  system: even a small NP phase  $\phi_s^{\text{NP}}$  implies considerable NP contributions to the mixing matrix element  $M_{12}^s$ .

### 3.4 Combined Constraints on NP through $\Delta M_d$ and $\phi_d$ : 2006 and 2010

We are now finally in a position to combine the constraints from both  $\Delta M_d$  and  $\phi_d$  to constrain the allowed region in the  $\sigma_d$ - $\kappa_d$  plane. The corresponding results are shown in Fig. 6, demonstrating the power of the contours described in the previous subsections for a transparent determination of  $\sigma_d$  and  $\kappa_d$ . We see that a non-vanishing value of  $\phi_d^{\text{NP}}$ , even as small as  $\phi_d^{\text{NP}} \approx -10^\circ$ , has a strong impact on the allowed space in the  $\sigma_d$ - $\kappa_d$  plane. In both scenarios with different lattice results and different values for  $|V_{ub}|$ , the upper bounds of  $\kappa_d \lesssim 2.5$  on the NP contributions following from the experimental value of  $\Delta M_d$  are reduced to  $\kappa_d \lesssim 0.5$ . Values of this order of magnitude are expected, for instance, on the basis of generic field-theoretical considerations [43, 47], as well as in a recently proposed framework for “next-to-minimal flavour violation” [49, 10].

In order to determine  $\kappa_d$  more precisely, it is mandatory to reduce the errors of  $\rho_d$ , which come from both  $\gamma$  and lattice calculations. As we noted above, the value of  $\gamma$  can be determined – with impressive accuracy – at the LHC [41], whereas progress on the lattice side is much harder to predict, but will hopefully be made. Assuming our benchmark scenario of Tab. 2, which corresponds to the lattice results of Eq. (11), the  $\sigma_d$ - $\kappa_d$  plane in 2010 looks like shown in Fig. 7 – and actually implies  $5\sigma$  evidence for NP from  $\phi_d^{\text{NP}} = -(9.8 \pm 2.0)^\circ$ . Although there is only a small allowed region left,  $\kappa_d$  is still only badly constrained; for an extraction with 10% uncertainty,  $f_{B_d} \hat{B}_{B_d}^{1/2}$  is required to 5% accuracy, i.e. the corresponding error in (11) has to be reduced by a factor of 2, which is the benchmark lattice theorists should strive for.

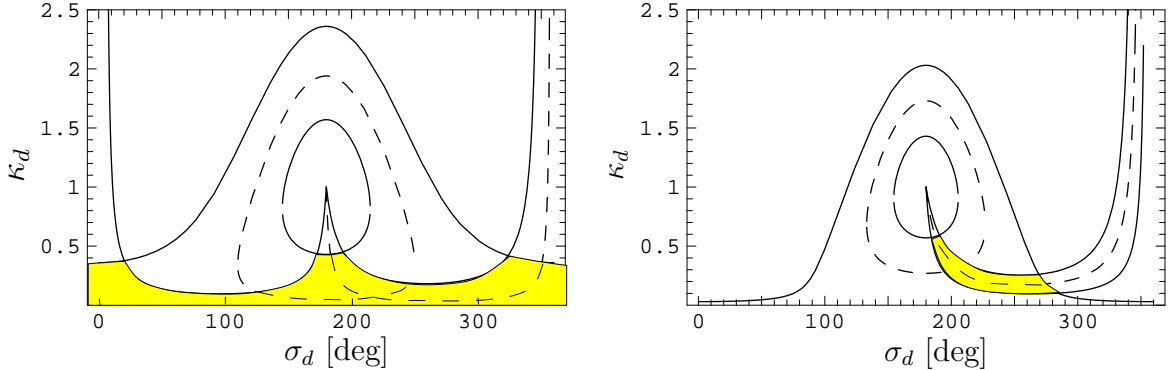


Figure 6: Left panel: allowed region (yellow/grey) in the  $\sigma_d$ - $\kappa_d$  plane in a scenario with the JLQCD lattice results (10) and  $\phi_d^{\text{NP}}|_{\text{excl}}$ . Dashed lines: central values of  $\rho_d$  and  $\phi_d^{\text{NP}}$ , solid lines:  $\pm 1\sigma$ . Right panel: ditto for the scenario with the (HP+JL)QCD lattice results (11) and  $\phi_d^{\text{NP}}|_{\text{incl}}$ .

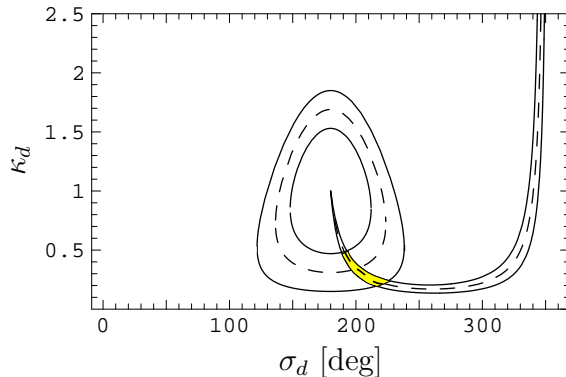


Figure 7: Allowed region in the  $\sigma_d$ - $\kappa_d$  plane (yellow/grey) in our 2010 scenario, using the parameters collected in Tab. 2 and  $\phi_d^{\text{NP}} = -(9.8 \pm 2.0)^\circ$ .

## 4 The $B_s$ -Meson System

### 4.1 Constraints on NP through $\Delta M_s$

Let us now have a closer look at the  $B_s$ -meson system. In order to describe NP effects in a model-independent way, we parametrize them analogously to (12) and (13). The relevant CKM factor is  $|V_{ts}^* V_{tb}|$ . Using once again the unitarity of the CKM matrix and including next-to-leading order terms in the Wolfenstein expansion as given in Ref. [34], we have

$$\left| \frac{V_{ts}}{V_{cb}} \right| = 1 - \frac{1}{2} (1 - 2R_b \cos \gamma) \lambda^2 + \mathcal{O}(\lambda^4). \quad (35)$$

Consequently, apart from the tiny correction in  $\lambda^2$ , the CKM factor for  $\Delta M_s$  is independent of  $\gamma$  and  $R_b$ , which is an important advantage in comparison with the  $B_d$ -meson system. The accuracy of the SM prediction of  $\Delta M_s$  is hence limited by the hadronic mixing parameter  $f_{B_s} \hat{B}_{B_s}^{1/2}$ . Using the numerical values discussed in Section 2, we obtain

$$\Delta M_s^{\text{SM}}|_{\text{JLQCD}} = (16.1 \pm 2.8) \text{ ps}^{-1},$$

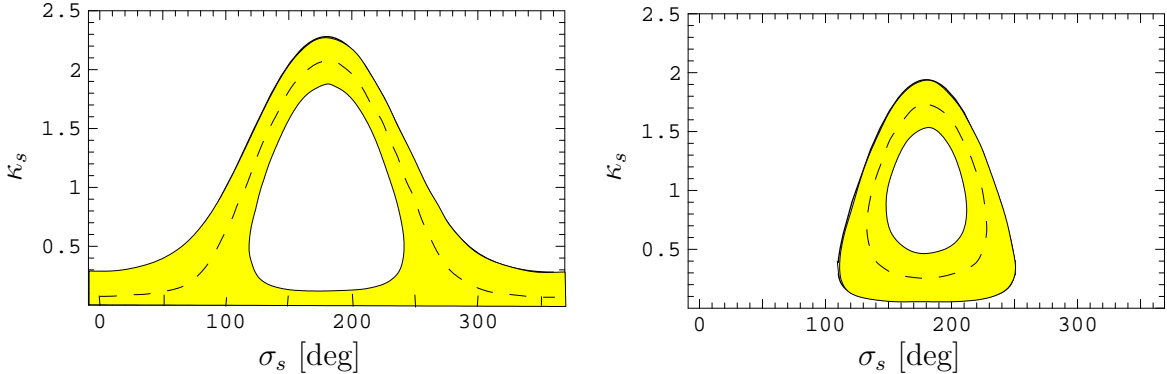


Figure 8: The allowed regions (yellow/grey) in the  $\sigma_s$ - $\kappa_s$  plane. Left panel: JLQCD lattice results (10). Right panel: (HP+JL)QCD lattice results (11).

$$\begin{aligned}
 \rho_s|_{\text{JLQCD}} &= 1.08_{-0.01}^{+0.03}(\text{exp}) \pm 0.19(\text{th}), \\
 \Delta M_s^{\text{SM}}|_{(\text{HP+JL})\text{QCD}} &= (23.4 \pm 3.8) \text{ ps}^{-1}, \\
 \rho_s|_{(\text{HP+JL})\text{QCD}} &= 0.74_{-0.01}^{+0.02}(\text{exp}) \pm 0.18(\text{th}), \tag{36}
 \end{aligned}$$

where we made the experimental and theoretical errors explicit. The values of  $\rho_s$ , which is defined in analogy to (14), refer to the CDF measurement of  $\Delta M_s$  in (4). These numbers are consistent with the SM case  $\rho_s = 1$ , but suffer from significant theoretical uncertainties, which are much larger than the experimental errors. Nevertheless, it is interesting to note that the (HP+JL)QCD result is  $1.5\sigma$  below the SM; a similar pattern arises in (25), though at the  $1\sigma$  level. Any more precise statement about the presence or absence of NP requires the reduction of theoretical uncertainties.

In Fig. 8, we show the constraints in the  $\sigma_s$ - $\kappa_s$  plane, which can be obtained from  $\rho_s$  with the help of the  $B_s$  counterpart of (15). We see that upper bounds of  $\kappa_s \lesssim 2.5$  arise from the measurement of  $\Delta M_s$ . In the case of (36), the bound on  $\sigma_s$  following from (16) would interestingly be effective, and imply  $110^\circ \leq \sigma_s \leq 250^\circ$ . Consequently, the CDF measurement of  $\Delta M_s$  leaves ample space for the NP parameters  $\sigma_s$  and  $\kappa_s$ . This situation will change significantly as soon as information about CP violation in the  $B_s$ -meson system becomes available. We shall return to this topic in Subsection 4.3.

## 4.2 Constraints on NP through $\Delta M_s$ and $\Delta M_d$

It is interesting to consider the ratio of  $\Delta M_s$  and  $\Delta M_d$ , which can be written as follows:

$$\frac{\Delta M_s}{\Delta M_d} = \frac{\rho_s}{\rho_d} \left| \frac{V_{ts}}{V_{td}} \right|^2 \frac{M_{B_s}}{M_{B_d}} \xi^2, \tag{37}$$

where the hadronic  $SU(3)$ -breaking parameter  $\xi$  is defined in Subsection 2.2. In the class of NP models with “minimal flavour violation” [50],<sup>3</sup> which contains also the SM, we have  $\rho_s/\rho_d = 1$ , so that (37) allows the extraction of the CKM factor  $|V_{ts}/V_{td}|$ , and hence  $|V_{td}|$ ,

<sup>3</sup>See Ref. [51] for a review, and Ref. [9] for a recent analysis addressing also the  $\Delta M_s$  measurement.

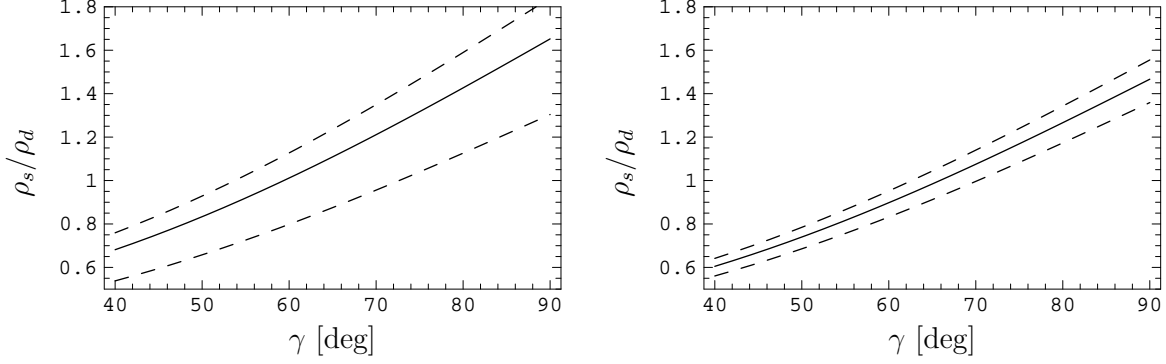


Figure 9: The dependence of  $\rho_s/\rho_d$  on  $\gamma$  for the central values of  $\Delta M_{d,s}$  in (4). Left panel: JLQCD results (10). Right panel: (HP+JL)QCD results (11). The plots are nearly independent of  $R_b$ .

as  $|V_{ts}|$  is known – to excellent accuracy – from (35). The advantage of this determination lies in the reduced theoretical uncertainty of  $\xi$  as compared to  $f_{B_d} \hat{B}_{B_d}^{1/2}$ .

In this paper, however, we turn the tables and constrain the ratio  $\rho_s/\rho_d$  through  $\Delta M_s/\Delta M_d$ . To this end, we express – in analogy to (17) – the UT side

$$R_t \equiv \frac{1}{\lambda} \left| \frac{V_{td}}{V_{cb}} \right| = \frac{1}{\lambda} \left| \frac{V_{td}}{V_{ts}} \right| \left[ 1 - \frac{1}{2} (1 - 2R_b \cos \gamma) \lambda^2 + \mathcal{O}(\lambda^4) \right] \quad (38)$$

in terms of  $R_b$  and  $\gamma$ :

$$R_t = \sqrt{1 - 2R_b \cos \gamma + R_b^2}, \quad (39)$$

allowing the determination of  $R_t$  through processes that are essentially unaffected by NP. The resulting value of  $R_t$  depends rather strongly on  $\gamma$ , which is the main source of uncertainty. Another determination of  $R_t$  that is independent of  $\gamma$  and  $R_b$  can, in principle, be obtained from radiative decays, in particular the ratio of branching ratios  $\mathcal{B}(B \rightarrow (\rho, \omega)\gamma)/\mathcal{B}(B \rightarrow K^*\gamma)$ , but is presently limited by experimental statistics; see Ref. [52] for a recent analysis.

Combining (37) and (38), we obtain the following expression for  $\rho_s/\rho_d$ :

$$\frac{\rho_s}{\rho_d} = \lambda^2 \left[ 1 - 2R_b \cos \gamma + R_b^2 \right] \left[ 1 + (1 - 2R_b \cos \gamma) \lambda^2 + \mathcal{O}(\lambda^4) \right] \frac{1}{\xi^2} \frac{M_{B_d}}{M_{B_s}} \frac{\Delta M_s}{\Delta M_d}. \quad (40)$$

In Fig. 9, we plot this ratio for the central values of  $\Delta M_d$  and  $\Delta M_s$  in (4), as a function of the UT angle  $\gamma$  for the values of  $\xi$  given in (10) and (11). We find that the corresponding curves are nearly independent of  $R_b$  and that  $\gamma$  is actually the key CKM parameter for the determination of  $\rho_s/\rho_d$ . The corresponding numerical values are given by:

$$\begin{aligned} \left. \frac{\rho_s}{\rho_d} \right|_{\text{JLQCD}} &= 1.11_{-0.01}^{+0.02}(\text{exp}) \pm 0.35(\gamma, R_b)_{-0.28}^{+0.12}(\xi), \\ \left. \frac{\rho_s}{\rho_d} \right|_{(\text{HP+JL})\text{QCD}} &= 0.99_{-0.01}^{+0.02}(\text{exp}) \pm 0.31(\gamma, R_b)_{-0.08}^{+0.06}(\xi). \end{aligned} \quad (41)$$



Because of the large range of allowed values of  $\gamma$ , Eq. (23), this ratio is currently not very stringently constrained. This situation should, however, improve significantly in the LHC era thanks to the impressive determination of  $\gamma$  to be obtained at the LHCb experiment. For our 2010 scenario as specified in Tab. 2, which corresponds to the right panel of Fig. 9 with  $\gamma = (70 \pm 5)^\circ$ , we find:

$$\left. \frac{\rho_s}{\rho_d} \right|_{2010} = 1.07 \pm 0.09(\gamma, R_b)_{-0.08}^{+0.06}(\xi) = 1.07 \pm 0.12, \quad (42)$$

where we made the errors arising from the uncertainties of  $\gamma$  and  $\xi$  explicit, and, in the last step, added them in quadrature. Consequently, the hadronic uncertainties and those induced by  $\gamma$  would now be of the same size, which should provide additional motivation for the lattice community to reduce the error of  $\xi$  even further. Despite the impressive reduction of uncertainty compared to the 2006 values in (41), the numerical value in (42) would still not allow a stringent test of whether  $\rho_s/\rho_d$  equals one: to establish a  $3\sigma$  deviation from 1, central values of  $\rho_s/\rho_d = 1.4$  or  $0.7$  would be needed. The assumed uncertainty of  $\gamma$  of  $5^\circ$  could also turn out to be too pessimistic, in which case even more progress would be needed from the lattice side to match the experimental accuracy.

The result in (42) would not necessarily suggest that there is no physics beyond the SM. In fact, and as can be seen from Tab. 2, the central values of  $\rho_d$  and  $\rho_s$  would both be smaller than one, i.e. would both deviate from the SM picture, although the hadronic uncertainties would again not allow us to draw definite conclusions. In order to shed further light on these possible NP contributions, the exploration of CP-violating effects in the  $B_s$ -meson system is essential.

### 4.3 CP Violation in the $B_s$ -System

To date, the CP-violating phase associated with  $B_s^0-\bar{B}_s^0$  mixing is completely unconstrained. In the SM, it is doubly Cabibbo-suppressed, and can be written as follows:

$$\phi_s^{\text{SM}} = -2\lambda^2\eta = -2\lambda^2R_b \sin \gamma \approx -2^\circ. \quad (43)$$

Here we used again (19) to express the Wolfenstein parameter  $\eta$  in terms of  $R_b$  and  $\gamma$ . Because of the small SM phase in (43),  $B_s^0-\bar{B}_s^0$  mixing is particularly well suited to search for NP effects, which may well lead to a sizeable value of  $\phi_s$  [53, 54]. In order to test the SM and probe CP-violating NP contributions to  $B_s^0-\bar{B}_s^0$  mixing, the decay  $B_s^0 \rightarrow J/\psi\phi$ , which is very accessible at the LHC [18], plays a key rôle. Thanks to mixing-induced CP violation in the time-dependent angular distribution of the  $J/\psi[\rightarrow \ell^+\ell^-]\phi[\rightarrow K^+K^-]$  decay products, the quantity

$$\sin \phi_s = \sin(-2\lambda^2R_b \sin \gamma + \phi_s^{\text{NP}}) \quad (44)$$

can be measured [55, 56], in analogy to the determination of  $\sin \phi_d$  through  $B_d^0 \rightarrow J/\psi K_s$ . After one year of data taking (which corresponds to  $2 \text{ fb}^{-1}$ ), LHCb expects a measurement with the statistical accuracy  $\sigma_{\text{stat}}(\sin \phi_s) \approx 0.031$ ; adding modes such as  $B_s \rightarrow J/\psi\eta, J/\psi\eta'$  and  $\eta_c\phi$ ,  $\sigma_{\text{stat}}(\sin \phi_s) \approx 0.013$  is expected after five years [41]. Also ATLAS and CMS will contribute to the measurement of  $\sin \phi_s$ , expecting uncertainties at the 0.1 level after one year of data taking, which corresponds to  $10 \text{ fb}^{-1}$  [57, 58].

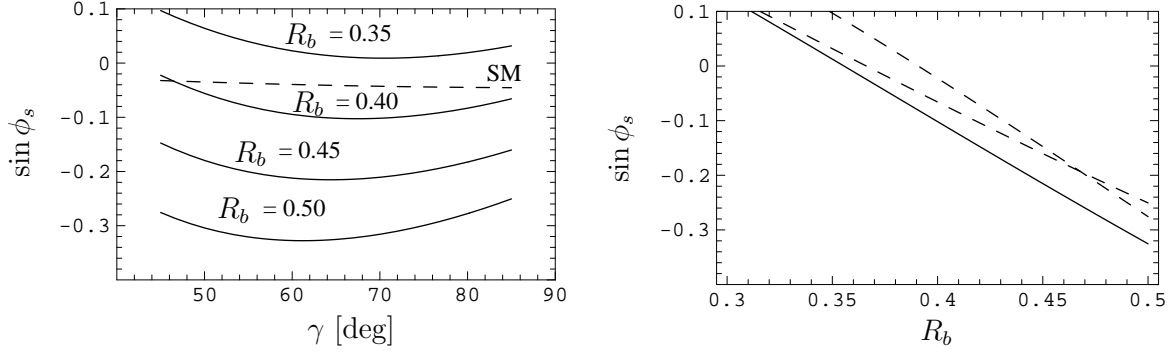


Figure 10:  $\sin \phi_s$  for a scenario with flavour-universal NP, i.e.  $\phi_s^{\text{NP}} = \phi_d^{\text{NP}}$ , as specified in Eq. (45), and  $\phi_d = 43.4^\circ$ . Left panel:  $\sin \phi_s$  as a function of  $\gamma$  for various values of  $R_b$ . Right panel:  $\sin \phi_s$  as a function of  $R_b$  for various values of  $\gamma$  (solid line:  $\gamma = 65^\circ$ , dashed lines:  $\gamma = (45^\circ, 85^\circ)$ ).

In order to illustrate the impact of NP effects, let us assume that the NP parameters satisfy the simple relation

$$\sigma_d = \sigma_s, \quad \kappa_d = \kappa_s, \quad (45)$$

i.e. that in particular  $\phi_d^{\text{NP}} = \phi_s^{\text{NP}}$ . This scenario would be supported by (42), although it would *not* belong to the class of models with MFV, as new sources of CP violation would be required. As we have seen in the previous section, the analysis of the  $B_d^0$  data for  $R_b^{\text{incl}} = 0.45$  indicates a small NP phase around  $-10^\circ$  in the  $B_d$ -system. In the above scenario, that would imply the presence of the same phase in the  $B_s$ -system, which would interfere constructively with the small SM phase and result in CP asymmetries at the level of  $-20\%$ . CP-violating effects of that size can easily be detected at the LHC. This exercise demonstrates again the great power of the  $B_s$ -meson system to reveal CP-violating NP contributions to  $B_q^0-\bar{B}_q^0$  mixing. The presence of a small NP phase could actually be considerably magnified, as illustrated in Fig. 10. In specific NP scenarios, also large CP-violating phases can still arise, and are in no way excluded by the CDF measurement of  $\Delta M_s$  in (4).

Let us finally also discuss the impact of CP violation measurements on the allowed region in the  $\sigma_s-\kappa_s$  plane in our 2010 scenario. To this end, we consider two cases:

- i)  $(\sin \phi_s)_{\text{exp}} = -0.04 \pm 0.02$ , in accordance with the SM;
- ii)  $(\sin \phi_s)_{\text{exp}} = -0.20 \pm 0.02$ , in accordance with the NP scenario of Fig. 10.

The measurement of  $\sin \phi_s$  implies a twofold solution for  $\phi_s$  and, therefore, also for  $\phi_s^{\text{NP}}$ . However, this ambiguity can be resolved through the determination of the sign of  $\cos \phi_s$ , which can be fixed through the strategies proposed in Ref. [55]. In Fig. 11, we show the situation in the  $\sigma_s-\kappa_s$  plane.<sup>4</sup> The dotted lines refer to negative values of  $\cos \phi_s$ . Assuming that these are experimentally excluded, we are left with strongly restricted regions, although  $\kappa_s$  could still take sizeable ranges, with upper bounds  $\kappa_s \approx 0.5$ . In the SM-like scenario, values of  $\sigma_s$  around  $180^\circ$  would arise, i.e. a NP contribution with

<sup>4</sup>The closed lines agree with those shown in the right panel of Fig. 8, as our 2010 scenario is based on the (HP+JL)QCD lattice results.

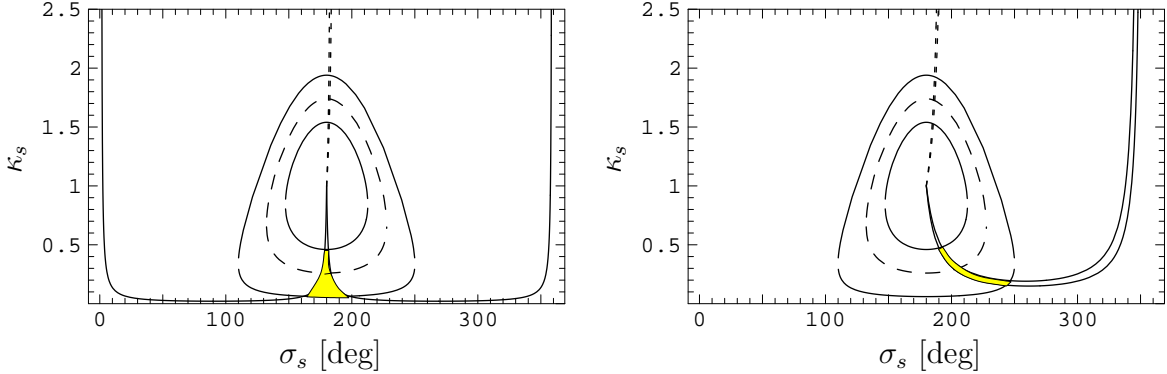


Figure 11: Combined constraints for the allowed region (yellow/grey) in the  $\sigma_s$ - $\kappa_s$  plane through  $\Delta M_s$  in (4) for the (HP+JL)QCD results (11) and CP violation measurements. Left panel: the SM scenario  $(\sin \phi_s)_{\text{exp}} = -0.04 \pm 0.02$ . Right panel: a NP scenario with  $(\sin \phi_s)_{\text{exp}} = -0.20 \pm 0.02$ . The solid lines correspond to  $\cos \phi_s > 0$ , the dotted lines to  $\cos \phi_s < 0$ .

a sign opposite to the SM. However, due to the absence of new CP-violating effects, the accuracy of lattice results would have to be considerably improved in order to allow the extraction of a value of  $\kappa_s$  incompatible with 0. On the other hand, a measurement of  $(\sin \phi_s)_{\text{exp}} = -0.20 \pm 0.02$  would give a NP signal at the  $10\sigma$  level, with  $\kappa_s \gtrsim 0.2$  from Eq. (28). In analogy to the discussion in Subsection 3.4, a determination of  $\kappa_s$  with 10% uncertainty requires  $f_{B_s} \hat{B}_{B_s}^{1/2}$  with 5% accuracy, i.e. the corresponding error in (11) has to be reduced by a factor of 2.

Since the discussion given so far does not refer to a specific model of NP, the question arises whether there are actually extensions of the SM that still allow large CP-violating NP phases in  $B_s^0$ - $\bar{B}_s^0$  mixing.

## 5 Specific Models of New Physics

In this section, we address the impact of the CDF measurement of  $\Delta M_s$  on two popular scenarios of NP, to wit

- an extra  $Z'$  boson with flavour non-diagonal couplings;
- generic effects in the minimal supersymmetric extension of the SM (MSSM) in the “mass insertion approximation”.

We would like to stress that our examples for NP scenarios should be viewed as illustrative rather than comprehensive and are not intended to compete with more dedicated analyses.

### 5.1 $Z'$ Gauge Boson with Non-Universal Couplings

Let us start with the effect of an extra  $U(1)'$  gauge boson  $Z'$ , which is the most simple application of the model-independent method discussed in Sections 3 and 4. The existence

of a new  $Z'$  gauge boson can induce FCNC processes at tree-level if the  $Z'$  coupling to physical fermions is non-diagonal. Such  $Z'$  bosons often occur, for instance, in the context of grand unified theories (GUTs), superstring theories, and theories with large extra dimensions, see, for instance, Refs. [59, 60]. In this paper, we illustrate the constraints on an extra  $Z'$  under the conditions that

- the  $Z$  couplings stay flavour diagonal, i.e.  $Z$ - $Z'$  mixing is negligible and the  $Z$  does not contribute to  $B$  mixing;
- the  $Z'$  has flavour non-diagonal couplings only to left-handed quarks, which means that its effect is described by only one complex parameter.

Note that the  $Z'$  contribution to  $B_s$  mixing is related to that for hadronic, leptonic and semileptonic decays in specific models where the  $Z'$  coupling to light quarks and leptons is known; in this paper, however, we treat the  $Z'$  in a model-independent way and assume its couplings to the  $b_L$  and  $s_L$  quark fields as independent. We only discuss the  $B_s$ -system and closely follow the notations of Ref. [61], where an earlier analysis of this scenario was given.

A purely left-handed off-diagonal  $Z'$  coupling to  $b$  and  $s$  quarks gives the following contribution to  $M_{12}^s$ .<sup>5</sup>

$$M_{12}^{s,Z'} = \frac{G_F}{\sqrt{2}} \rho_L^2 e^{2i\phi_L} \frac{4}{3} \hat{\eta}^B \hat{B}_{B_s} f_{B_s}^2 M_{B_s}, \quad (46)$$

where  $\rho_L e^{i\phi_L} \equiv (g' M_Z)/(g M_{Z'}) B_{sb}^L$  is defined in terms of the SM  $U_Y(1)$  gauge coupling  $g$ , the  $U(1)'$  coupling  $g'$ , the respective gauge boson masses  $M_{Z,Z'}$  and the FCNC coupling  $B_{sb}^L$  of the  $Z'$  to  $b_L$  and  $s_L$ . Generically, one would expect  $g/g' = \mathcal{O}(1)$ , if both  $U(1)$  groups have the same origin, for instance in a GUT framework, and  $M_Z/M_{Z'} = \mathcal{O}(0.1)$  for a TeV-scale  $Z'$ . If in addition the size of the  $Z'$  couplings  $B^L$  is set by the quarks' Yukawa couplings, one also expects  $|B_{sb}^L| \approx |V_{ts}^* V_{tb}|$  and  $\rho_L = \mathcal{O}(10^{-3})$ .

The impact of the CDF measurement of  $\Delta M_s$  on this model can be directly read off Fig. 8 through the identifications

$$\rho_L \leftrightarrow (\kappa_s/f)^{1/2}, \quad \phi_L \leftrightarrow \sigma_s/2,$$

with

$$f = \frac{16\pi^2}{\sqrt{2}} \frac{1}{G_F M_W^2 S_0(x_t) |V_{ts}|^2} = (3.57 \pm 0.01) \cdot 10^5.$$

Presently, values of  $\kappa_s$  as large as 2.5 are still allowed, see Fig. 8, which corresponds to

$$\rho_L < 2.6 \cdot 10^{-3}. \quad (47)$$

If a non-zero value of the NP phase  $\phi_s^{\text{NP}}$  should be measured at the LHC, this value can be immediately translated into a lower bound on  $\rho_L$ , using (28). Assuming  $\phi_s^{\text{NP}} = -10^\circ$ , one has

$$\sin \phi_s = -0.2 \leftrightarrow \rho_L > 0.5 \cdot 10^{-3}, \quad (48)$$

---

<sup>5</sup>Strictly speaking,  $\hat{\eta}^B \hat{B}_{B_s}$  should be taken at LO accuracy; here, we effectively absorb the (small) difference between LO and NLO expressions into the definition of  $\rho_L$ .

and  $\kappa_s < 0.5 \leftrightarrow \rho_L < 1.2 \cdot 10^{-3}$ . Any more precise constraint on  $\rho_L$  will depend on the progress in lattice determinations of  $f_{B_s} \hat{B}_{B_s}^{1/2}$ .

The upper bound on  $\rho_L$  given in Eq. (47) can be converted into a lower bound on the  $Z'$  mass:

$$1.5 \text{ TeV} \left( \frac{g'}{g} \right) \left| \frac{B_{sb}^L}{V_{ts}} \right| < M_{Z'}. \quad (49)$$

In the scenario of (48), there is also an upper bound and the lower bound is raised:

$$3 \text{ TeV} \left( \frac{g'}{g} \right) \left| \frac{B_{sb}^L}{V_{ts}} \right| < M_{Z'} < 7.5 \text{ TeV} \left( \frac{g'}{g} \right) \left| \frac{B_{sb}^L}{V_{ts}} \right|. \quad (50)$$

We would like to stress again that these bounds apply to a model where the  $Z'$  has flavour non-diagonal couplings only to left-handed quarks. Eq. (50) can be compared to the existing lower bounds on the  $Z'$  mass from direct searches, as for instance quoted by CDF [62]; these limits are model-dependent, but in the ballpark of  $\sim 800 \text{ GeV}$ , which is perfectly compatible with (50). On the other hand, if a  $Z'$  was found in direct searches at the Tevatron or the LHC, the bounds on  $\rho_L$  would constrain its couplings. This is particularly interesting in a framework with nearly family-universal couplings and illustrates the potential synergy between direct searches for NP and constraints from flavour physics.

Note that (47) can also be translated into an upper bound on the branching ratio of  $B_s \rightarrow \mu^+ \mu^-$ , at least if the coupling of the  $Z'$  to  $\mu^+ \mu^-$  is known. The relevance of such a bound is not quite clear, however, since we have set the coupling of the  $Z'$  to right-handed fermions to 0.

## 5.2 MSSM in the Mass Insertion Approximation

Let us now discuss  $B$  mixing in supersymmetry. Whereas in the SM flavour violation is parametrized by the CKM matrix, in SUSY there are many more possible ways in which both lepton and quark flavours can change. This is because scalar quarks and leptons carry the flavour quantum numbers of their SUSY partners, which implies that flavour violation in the scalar sector can lead to flavour violation in the observed fermionic sector of the theory. The parameters controlling flavour violation in the MSSM are quite numerous – there are about 100 soft SUSY breaking parameters which could give rise to huge – and unobserved – flavour violation. One way to defuse this so-called SUSY flavour problem is to assume that the squark (and slepton) masses are approximately aligned with the quark (and lepton) masses. “Alignment” means that, in the basis of physical states, where the fermion masses are diagonal, the scalar mass matrices are approximately diagonal as well. In this case, one can treat the off-diagonal terms in the sfermion mass matrices,

$$(\delta_{ij}^f)_{AB} \equiv (\Delta m_{ij}^2)_{AB} / m_{\tilde{f}}^2,$$

as perturbations. Here  $i, j = 1, 2, 3$  are family indices,  $A, B = L, R$  refers to the “chirality” of the sfermions<sup>6</sup> and  $m_{\tilde{f}}$  is the average sfermion mass. This so-called mass insertion approximation (MIA) has been first introduced in Ref. [63], and was extensively applied

---

<sup>6</sup>Sfermions are scalar particles and hence have no chirality; the labels  $L$  and  $R$  refer to the fact that they are the SUSY partners of left- and right-handed quark fields, respectively.

to FCNC and CP-violating phenomena in Ref. [64]. Its strength is the fact that it is independent of specific model assumptions on the values of soft SUSY-breaking parameters, but its weakness is that there are many free parameters, so there is a certain loss of predictive power. In this paper, we do not attempt a sophisticated analysis, which will only be possible once a full NLO calculation of the corresponding short-distance functions has become available, which is in preparation, see Ref. [65]. Rather, we would like to illustrate the impact of the constraints from  $\Delta M_s$  on the dominant mass insertions, along the lines of, for instance, Refs. [66, 8]. Bounds on mass insertions from  $B_d$  mixing have been investigated in Ref. [67].

In supersymmetric theories the effective Hamiltonian  $\mathcal{H}_{\text{eff}}^{\Delta B=2}$  responsible for  $B$  mixing, see Eq. (1), is generated by the SM box diagrams with  $W$  exchange and box diagrams mediated by charged Higgs, neutralino, photino, gluino and chargino exchange. For small values of  $\tan \beta_{\text{SUSY}}$ , which is the ratio of vacuum expectation values of the two MSSM Higgs doublets, the Higgs contributions are suppressed by the quark masses and can be neglected. Photino and neutralino diagrams are also heavily suppressed compared to those from gluino and chargino exchange, due to the smallness of the electroweak couplings compared to  $\alpha_s$ . The gluino contribution was calculated in Ref. [64], the chargino one in Ref. [68]. The analysis of Ref. [66] has shown that the chargino contributions are also very small, so that the  $B_s^0-\bar{B}_s^0$  transition matrix element is given, to good accuracy, by

$$M_{12}^s = M_{12}^{s,\text{SM}} + M_{12}^{s,\tilde{g}}, \quad (51)$$

where  $M_{12}^{s,\text{SM}}$  and  $M_{12}^{s,\tilde{g}}$  indicate the SM and gluino contributions, respectively. It turns out that the largest contribution to  $M_{12}^{s,\tilde{g}}$  comes from terms in  $(\delta_{23}^d)_{LL}(\delta_{23}^d)_{RR}$ , whereas chirality flipping  $LR$  and  $RL$  mass insertions are only poorly constrained from  $B_s$  mixing, but dominantly enter  $b \rightarrow s\gamma$  decays. The bounds on  $(\delta_{23}^d)_{LR}$  and  $(\delta_{23}^d)_{RL}$  posed by the corresponding branching ratio have been investigated in Ref. [69], a recent update can be found in Ref. [70]. As for the chirality-conserving mass insertions, the impact of the D0 bound (5) has been studied in Refs. [6, 8]. Here we set all but one mass insertion to 0 and restrict ourselves to bounds on  $(\delta_{23}^d)_{LL}$  and the impact of a future measurement of  $\phi_s$  on these bounds.

The effective  $\Delta B = 2$  Hamiltonian in the MSSM contains a total of eight operators as compared to only one in the SM. The corresponding hadronic matrix elements (bag parameters) have been calculated, in quenched approximation, in Ref. [71]. The evolution of the Wilson coefficients from  $M_S$ , the scale where the SUSY particles are integrated out, to  $m_b$  is known to next-to-leading order [72, 67]. The expression for  $\Delta M_s$  in the MSSM then depends on  $M_S$ ,  $m_{\tilde{q}}$ , the average sfermion mass, and  $m_{\tilde{g}}$ , the gluonino mass. We take  $m_{\tilde{q}} = 500 \text{ GeV} = m_{\tilde{g}}$  and also  $M_S = 500 \text{ GeV}$  as illustrative values. We then obtain the constraints on  $\text{Re}(\delta_{23}^d)_{LL}$  and  $\text{Im}(\delta_{23}^d)_{LL}$  shown in Fig. 12. The closed curves in the centre of the plots correspond to the allowed values of the real and imaginary part of  $(\delta_{23}^d)_{LL}$  after the measurement of  $\Delta M_s$ ; note that the experimental value of  $\Delta M_s$  is incompatible with the SM prediction at  $1.5\sigma$  level when the (HP+JL)QCD lattice data are used, Eq. (36), hence the origin is excluded in the right panel. The open lines correspond to constraints imposed by a measurement of the mixing phase  $\phi_s$ , as explained in the caption. It is obvious that at present no value of  $\phi_s$  is excluded and that the precise measurement of the mixing phase, expected to take place at the LHC, will considerably restrict the parameter space of SUSY mass insertions.

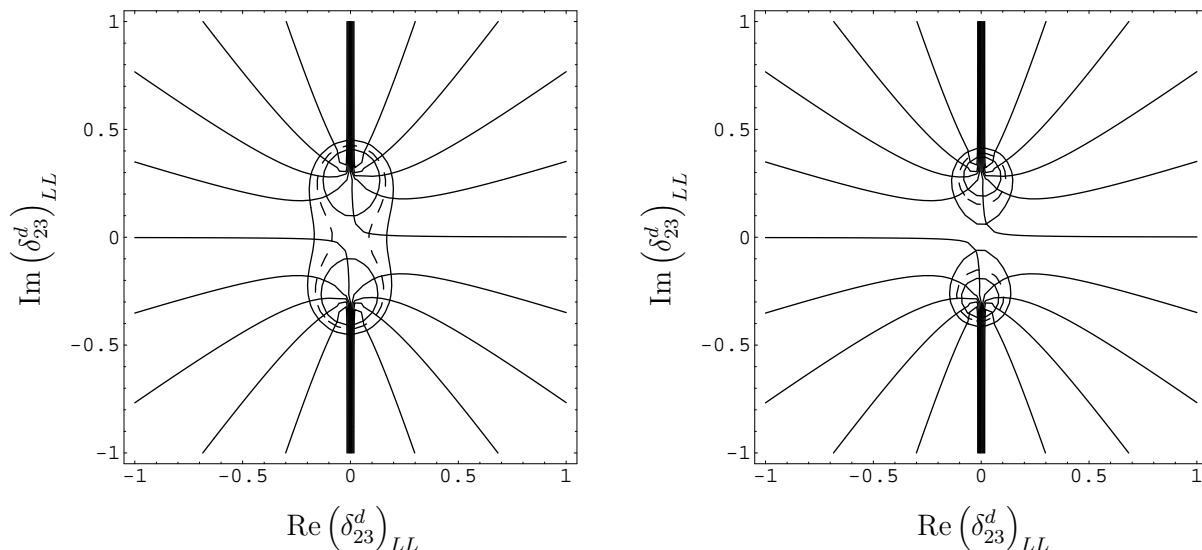


Figure 12:  $1\sigma$  constraints on  $(\delta_{23}^d)_{LL}$  from  $\Delta M_s$  (closed lines). Left panel: JLQCD results (10), right panel: (HP+JL)QCD results (11). The open lines denote constraints posed by a measurement of  $\phi_s$ : the curves in the upper right and lower left quadrant correspond, from bottom to top in the upper quadrant, and top to bottom in the lower quadrant, to  $\phi_s \in \{0^\circ, 36^\circ, 72^\circ, 108^\circ, 144^\circ\}$ , whereas those in the upper left and lower right quadrant correspond to phases between  $-180^\circ$  and  $0^\circ$ .

If SUSY is found at the LHC, and the gluino and average squark masses are measured, the results from MIA analyses of flavour processes will help to constrain the soft SUSY breaking terms and hence the – yet to be understood – mechanism of SUSY breaking. Given the sheer number of these terms (about 100), it will be very difficult to resolve the richness of SUSY breaking from direct SUSY searches alone, which will have to be complemented by constraints (or measurements) from flavour physics – which, in turn, will become more expressive, once the direct searches will have provided the relevant mass scales.

## 6 Conclusions and Outlook

The FCNC processes of  $B_d^0-\bar{B}_d^0$  and  $B_s^0-\bar{B}_s^0$  mixing offer interesting probes to search for signals of physics beyond the SM. Although the former phenomenon is well established since many years, the latter has only just been observed at the Tevatron, thereby raising in particular the question of the implications for the parameter space of NP.

The current situation can be summarized as follows: the experimental value of the mass difference  $\Delta M_d$  and the recently measured  $\Delta M_s$  agree with the SM. However, the SM predictions of these quantities suffer from large uncertainties. In particular, some lattice calculations ((HP+JL)QCD) indicate a value of  $\Delta M_s^{\text{SM}}$  that is  $1.5\sigma$  larger than the experimental CDF value, whereas the JLQCD results show no such effect. A similar pattern arises at the  $1\sigma$  level in the  $B_d$ -meson system. In view of these uncertainties, values

of  $\kappa_{d,s}$ , the strength of the NP contributions to  $B_{d,s}$  mixing, as large as 2.5 are still allowed by the experimental values of  $\Delta M_{d,s}$ , and the new CP-violating phases  $\sigma_{d,s}$  are essentially unconstrained. Complementary information is provided by CP violation. Interestingly, the impressive measurement of mixing-induced CP violation in  $B_d^0 \rightarrow J/\psi K_S$  (and similar modes) at the  $B$  factories may indicate a small – but noticeable – CP-violating NP phase  $\phi_d^{\text{NP}}$  around  $-10^\circ$ , which would have a drastic impact on the allowed region in the  $\sigma_d$ – $\kappa_d$  plane and would result in a lower bound on  $\kappa_d$  of  $\approx 0.2$ . In any case, the experimentally excluded large values of  $\phi_d^{\text{NP}}$  reduce the upper bound  $\kappa_d \approx 2.5$  significantly to 0.5. On the other hand, no information about  $\phi_s^{\text{NP}}$  is currently available, so that we are left with the large range of  $0 \lesssim \kappa_s \lesssim 2.5$ .

The following quantities play a key rôle for these studies: mixing:

- The CKM parameters  $\gamma$  and  $R_b \propto |V_{ub}/V_{cb}|$ , which enter the analysis of  $B_d^0$ – $\bar{B}_d^0$  mixing in a complementary manner. Whereas the UT angle  $\gamma$  is currently a significant source of uncertainty for the SM prediction of  $\Delta M_d$  (and  $\Delta M_s/\Delta M_d$ ),  $R_b$  is crucial for the detection of a NP phase  $\phi_d^{\text{NP}}$ . Thanks to the LHCb experiment, the situation for  $\gamma$  will improve dramatically in the future, where we assumed  $\gamma = (70 \pm 5)^\circ$  in our 2010 benchmark scenario. Concerning  $R_b$ , the error of  $|V_{cb}|$  has already a marginal impact. However, there is currently a  $1\sigma$  discrepancy between the inclusive and exclusive determinations of  $|V_{ub}|$ , pointing towards  $\phi_d^{\text{NP}} \approx -10^\circ$  and  $\phi_d^{\text{NP}} \approx 0^\circ$ , respectively. Consequently, it is crucial to clarify this situation and to reduce the uncertainty of  $|V_{ub}|$ . In our benchmark scenario, we assume that the central value of  $|V_{ub}|_{\text{incl}}$  will be confirmed, and that its uncertainty shrinks to 5% due to experimental and theoretical progress. It is an advantage of the  $B_s$ -meson system that the SM analysis of its mixing parameters is essentially unaffected by CKM uncertainties.
- The hadronic parameters  $f_{B_q} \hat{B}_{B_q}^{1/2}$ , which enter the SM predictions of  $\Delta M_q$ . For a determination of  $\kappa_q$  with 10% uncertainty, the errors of the (HP+JL)QCD lattice results have to be reduced by a factor of 2. The hadronic uncertainties are smaller if one considers the ratio  $\Delta M_s/\Delta M_d$ , involving the  $SU(3)$ -breaking parameter  $\xi$ . Presently, there is no indication of this ratio to deviate from its SM prediction, but there is still a large uncertainty. In our 2010 benchmark scenario, the error from  $\xi$  would match that from  $\gamma$ . Nevertheless, it will probably be challenging to detect NP through deviations of  $\rho_s/\rho_d$  from 1. Moreover, a result in agreement with 1 does not allow any conclusion about the presence or absence of NP, as  $\rho_s$  and  $\rho_d$  may both deviate similarly from 1, except for excluding certain NP scenarios, like for instance Higgs penguins enhanced by large values of  $\tan \beta_{\text{SUSY}}$ .

Concerning the prospects for the search for NP through  $B_s^0$ – $\bar{B}_s^0$  mixing at the LHC, it will be very challenging if essentially no CP-violating effects will be found in  $B_s^0 \rightarrow J/\psi\phi$  (and similar decays). On the other hand, as we demonstrated in our analysis, even a small phase  $\phi_s^{\text{NP}} \approx -10^\circ$  (inspired by the  $B_d$  data) would lead to CP asymmetries at the  $-20\%$  level, which could be unambiguously detected after a couple of years of data taking, and would not be affected by hadronic uncertainties. Conversely, the measurement of such an asymmetry would allow one to establish lower bounds on the strength of NP contribution – even if hadronic uncertainties still preclude a direct extraction of this contribution from  $\Delta M_s$  – and to dramatically reduce the allowed region in the NP parameter space. In fact,



the situation may be even more promising, as specific scenarios of NP still allow large new phases in  $B_s^0-\bar{B}_s^0$  mixing, also after the measurement of  $\Delta M_s$ . We have illustrated this exciting feature by considering models with an extra  $Z'$  boson and SUSY scenarios with an approximate alignment of quark and squark masses.

In essence, the lesson to be learnt from the CDF measurement of  $\Delta M_s$  is that NP may actually be hiding in  $B_s^0-\bar{B}_s^0$  mixing, but is still obscured by parameter uncertainties, some of which will be reduced by improved statistics at the LHC, whereas others require dedicated work of, in particular, lattice theorists. The smoking gun for the presence of NP in  $B_s^0-\bar{B}_s^0$  mixing will be the detection of a non-vanishing value of  $\phi_s^{\text{NP}}$  through CP violation in  $B_s^0 \rightarrow J/\psi\phi$ . Let us finally emphasize that the current  $B$ -factory data may show – in addition to  $\phi_d^{\text{NP}} \approx -10^\circ$  – other first indications of new sources of CP violation through measurements of  $B_d^0 \rightarrow \phi K_S$  and  $B \rightarrow \pi K$  decays, which may point towards a modified electroweak penguin sector. All these examples are yet another demonstration that flavour physics is not an optional extra, but an indispensable ingredient in the pursuit of NP, also and in particular in the era of the LHC.

## Acknowledgements

We would like to thank Martin Lüscher for a discussion of the current status of lattice calculations of  $B$  mixing parameters.

## References

- [1] E. Barberio *et al.* [HFAG], hep-ex/0603003; updated results available at <http://www.slac.stanford.edu/xorg/hfag/>.
- [2]  $B$  Oscillations Working Group: <http://lepbosec.web.cern.ch/LEPBOSC/>.
- [3] G. Gomez-Ceballos [CDF coll.], talk at FPCP 2006, <http://fpcp2006.triumf.ca>.
- [4] V. Abazov *et al.* [D0 coll.], hep-ex/0603029.
- [5] M. Carena *et al.*, hep-ph/0603106.
- [6] M. Ciuchini and L. Silvestrini, hep-ph/0603114.
- [7] L. Velasco-Sevilla, hep-ph/0603115.
- [8] M. Endo and S. Mishima, hep-ph/0603251.
- [9] M. Blanke, A.J. Buras, D. Guadagnoli and C. Tarantino, hep-ph/0604057.
- [10] Z. Ligeti, M. Papucci and G. Perez, hep-ph/0604112.
- [11] J. Foster, K.I. Okumura and L. Roszkowski, hep-ph/0604121.
- [12] G. Buchalla, A.J. Buras and M.E. Lautenbacher, *Rev. Mod. Phys.* **68** (1996) 1125.

- [13] N. Cabibbo, *Phys. Rev. Lett.* **10** (1963) 531.
- [14] M. Kobayashi and T. Maskawa, *Prog. Theor. Phys.* **49** (1973) 652.
- [15] Tevatron Electroweak Working Group, hep-ex/0507091.
- [16] T. Inami and C.S. Lim, *Prog. Theor. Phys.* **65** (1981) 297 [E: **65** (1981) 1772].
- [17] S.L. Glashow, J. Iliopoulos and L. Maiani, *Phys. Rev.* **D2** (1970) 1285.
- [18] P. Ball *et al.*, hep-ph/0003238.
- [19] L. Wolfenstein, *Phys. Rev. Lett.* **51** (1983) 1945.
- [20] S. Eidelman *et al.* [Particle Data Group], *Phys. Lett.* **B592** (2004) 1.
- [21] R. Fleischer, *Phys. Rept.* **370** (2002) 537.
- [22] O. Buchmüller and H. Flücher, hep-ph/0507253.
- [23] P. Gambino and N. Uraltsev, *Eur. Phys. J.* **C34** (2004) 181.
- [24] M. Okamoto *et al.*, *Nucl. Phys. Proc. Suppl.* **140** (2005) 461;  
E. Gulez *et al.*, *Phys. Rev.* **D73** (2006) 074502.
- [25] A. Khodjamirian *et al.*, *Phys. Rev.* **D62** (2000) 114002;  
P. Ball and R. Zwicky, *JHEP* **0110** (2001) 019; *Phys. Rev.* **D71** (2005) 014015; *Phys. Rev.* **D71** (2005) 014029; *Phys. Lett.* **B625** (2005) 225.
- [26] J.R. Andersen and E. Gardi, *JHEP* **0601** (2006) 097.
- [27] H. Leutwyler, *Phys. Lett.* **B378** (1996) 313.
- [28] A.S. Kronfeld and S.M. Ryan, *Phys. Lett.* **B543** (2002) 59.
- [29] S. Aoki *et al.* [JLQCD coll.], *Phys. Rev. Lett.* **91** (2003) 212001.
- [30] A. Gray *et al.* [HPQCD coll.], *Phys. Rev. Lett.* **95** (2005) 212001.
- [31] M. Okamoto, *PoS LAT2005* (2005) 013.
- [32] F. Palombi, M. Papinutto, C. Pena and H. Wittig [ALPHA coll.], *PoS LAT2005* (2005) 214.
- [33] M. Creutz, hep-lat/0603020;  
C. Bernard, M. Golterman, Y. Shamir and S. Sharpe, hep-lat/0603027;  
C. Bernard, M. Golterman and Y. Shamir, hep-lat/0604017.
- [34] A.J. Buras, M.E. Lautenbacher and G. Ostermaier, *Phys. Rev.* **D50** (1994) 3433.
- [35] E. Blucher *et al.*, hep-ph/0512039.
- [36] G. Cavoto *et al.*, hep-ph/0603019.

- [37] J. Charles *et al.* [CKMfitter Group], *Eur. Phys. J.* **C41** (2005) 1; for the most recent updates, see <http://ckmfitter.in2p3.fr/>.
- [38] M. Bona *et al.* [UTfit Collaboration], *JHEP* **0507** (2005) 028; for the most recent updates, see <http://utfit.roma1.infn.it/>.
- [39] A.J. Buras, R. Fleischer, S. Recksiegel and F. Schwab, *Eur. Phys. J.* **C45** (2006) 701.
- [40] C.W. Bauer, I.Z. Rothstein and I.W. Stewart, *Phys. Rev. Lett.* **94** (2005) 231802; hep-ph/0510241.
- [41] O. Schneider, talk at the “Flavour in the era of the LHC” workshop, CERN, November 2005, <http://cern.ch/flavlhc>.
- [42] A.B. Carter and A.I. Sanda, *Phys. Rev. Lett.* **45** (1980) 952; *Phys. Rev.* **D23** (1981) 1567;  
I.I. Bigi and A.I. Sanda, *Nucl. Phys.* **B193** (1981) 85.
- [43] R. Fleischer and T. Mannel, *Phys. Lett.* **B506** (2001) 311.
- [44] R. Fleischer, *J. Phys.* **G32** (2006) R71.
- [45] R. Fleischer, *Phys. Lett.* **B562** (2003) 234; *Nucl. Phys.* **B659** (2003) 321.
- [46] R. Fleischer and J. Matias, *Phys. Rev.* **D66** (2002) 054009.
- [47] R. Fleischer, G. Isidori and J. Matias, *JHEP* **0305** (2003) 053.
- [48] M. Bona *et al.* [UTfit Collaboration], *JHEP* **0603** (2006) 080.
- [49] K. Agashe, M. Papucci, G. Perez and D. Pirjol, hep-ph/0509117.
- [50] G. D’Ambrosio, G.F. Giudice, G. Isidori and A. Strumia, *Nucl. Phys.* **B645** (2002) 155;  
A.J. Buras *et al.*, *Phys. Lett.* **B500** (2001) 161.
- [51] A.J. Buras, *Acta Phys. Polon.* **B34** (2003) 5615.
- [52] P. Ball and R. Zwicky, *JHEP* **0604** (2006) 046.
- [53] Y. Nir and D.J. Silverman, *Nucl. Phys.* **B345** (1990) 301.
- [54] G.C. Branco, T. Morozumi, P.A. Parada and M.N. Rebelo, *Phys. Rev.* **D48** (1993) 1167.
- [55] I. Dunietz, R. Fleischer and U. Nierste, *Phys. Rev.* **D63** (2001) 114015.
- [56] A.S. Dighe, I. Dunietz and R. Fleischer, *Eur. Phys. J.* **C6** (1999) 647.
- [57] M. Smizanska (ATLAS collaboration), private communication.

- [58] T. Speer (CMS collaboration), private communication.
- [59] P. Langacker and M. Plümacher, *Phys. Rev.* **D62** (2000) 013006.
- [60] M. Cvetič, G. Shiu and A.M. Uranga, *Phys. Rev. Lett.* **87** (2001) 201801; *Nucl. Phys.* **B615** (2001) 3;  
M. Cvetič, P. Langacker and G. Shiu, *Phys. Rev.* **D66** (2002) 066004.
- [61] V. Barger, C.W. Chiang, J. Jiang and P. Langacker, *Phys. Lett.* **B596** (2004) 229.
- [62] A. Abulencia *et al.* [CDF coll.], hep-ex/0602045; hep-ex/0603006.
- [63] L.J. Hall, V.A. Kostelecky and S. Raby, *Nucl. Phys.* **B267** (1986) 415.
- [64] F. Gabbiani *et al.*, *Nucl. Phys.* **B477** (1996) 321.
- [65] M. Ciuchini *et al.*, *PoS HEP2005* (2006) 221.
- [66] P. Ball, S. Khalil and E. Kou, *Phys. Rev.* **D69** (2004) 115011.
- [67] D. Becirevic *et al.*, *Nucl. Phys.* **B634** (2002) 105.
- [68] E. Gabrielli and S. Khalil, *Phys. Rev.* **D67** (2003) 015008.
- [69] M. Ciuchini, E. Franco, A. Masiero and L. Silvestrini, *Phys. Rev.* **D67** (2003) 075016  
[E: **D68** (2003) 079901].
- [70] L. Silvestrini, hep-ph/0510077.
- [71] D. Becirevic *et al.*, *JHEP* **0204** (2002) 025.
- [72] A.J. Buras, S. Jäger and J. Urban, *Nucl. Phys.* **B605** (2001) 600.